

Data-Driven Greenhouse Climate Regulation in Lettuce Cultivation Using BiLSTM and GRU Predictive Control

Soumo Emmanuel Arnaud^{*,a}, Marcello Calisti^b, Athanasios Polydoros^a

^a*University of Lincoln, School of Engineering, Physical Science and Lincoln Centre for Autonomous Systems, , Lincoln, LN6 7TS, , United Kingdom*

^b*Sant'Anna School of Advanced Studies, The BioRobotics Institute, Viale Rinaldo Piaggio 34, Pontedera, , Pisa, Italy*

Abstract

Efficient greenhouse management is essential for sustainable food production in response to a growing global population. However, maintaining optimal indoor climates requires significant energy and resources, making advanced control systems critical for economic viability and environmental sustainability. Traditional greenhouse models are often complex and imprecise, limiting the effectiveness of conventional control strategies. To address these challenges, this study investigates data-driven predictive control methods using Gated Recurrent Unit (GRU) and Long Short-Term Memory (LSTM) neural networks. Our experiments showed that GRU-based predictive control reduced temperature and humidity violations by up to 5% and required 40% less computation time than the LSTM approach, all while maintaining equivalent economic performance and crop yield. These findings demonstrate that GRU-based predictive control offers a more efficient and practical solution for real-time greenhouse climate regulation in precision agriculture.

Keywords: Greenhouse climate control, Model Predictive Control (MPC), Data-driven modeling, Long Short-Term Memory (LSTM), Gated Recurrent Unit (GRU), Deep learning, Precision agriculture, Energy-efficient control, Predictive control, Crop yield optimization

1. INTRODUCTION

Global food security faces significant challenges. The number of undernourished people has been steadily increasing since 2014, reaching an estimated 720 to 811 million in 2020 [6]. This rise occurs as the world population,

currently around 7.7 billion, is projected to reach 9.7 billion by 2050, driving a rapid increase in demand for fresh, nutritious food [4]. Consequently, food production must increase by approximately 70% between 2005 and 2050 to meet future needs [5]. At the same time, critical resources such as freshwater [7], fossil fuels, and arable land are becoming increasingly scarce, while the impacts of climate change continue to intensify. As a result, producing high-quality, fresh food in a resource-efficient manner is more important than ever. Greenhouse cultivation has emerged as a powerful approach to agricultural intensification. Studies indicate that it can achieve substantial yield increases, typically ranging from 10% to 20%, while simultaneously reducing critical resource inputs by 25% to 35% [8, 10]. These considerable benefits have contributed to the accelerated global growth of protected horticulture. Nevertheless, the widespread adoption of greenhouse technologies is constrained by inherent challenges, notably their high energy demands and the significant initial capital investments required [9].

Greenhouses are essential for crop cultivation, as they provide a controlled environment that shields plants from unpredictable outdoor weather. In today's world where energy costs are rising and labor and resources are becoming increasingly scarce, efficient and automated greenhouse management is more important than ever. This approach helps maximize crop production while minimizing resource use. However, outdoor weather constitutes a significant disturbance, making it challenging to control the greenhouse climate, develop accurate models, and optimize operations for optimal performance [3]. A greenhouse is a complex system consisting of two primary components: the cultivated plants and the surrounding controlled environment. This internal environment is influenced by a combination of external weather conditions, the functioning of greenhouse equipment, and the physiological activities of the plants themselves. To understand, predict, and optimize the behavior of such systems, researchers commonly rely on mathematical modeling. These models serve a dual purpose: they offer insights into the underlying physical and biological processes and support the development of control strategies to enhance system performance [1, 2].

Traditional greenhouse modeling approaches are typically deterministic and based on first-principles, drawing from established scientific understanding of plant physiology, thermodynamics, and fluid dynamics [34, 33]. Although these models can provide detailed and mechanistic insights, they are often complex, featuring nonlinear dynamics and a large number of parameters that have to be manually tuned. This complexity reduces their adaptability

to different greenhouse setups or operational conditions. Furthermore, first-principles models are generally limited in their ability to handle uncertainty, as estimating the variability in model parameters requires extensive datasets and computationally demanding statistical methods. While these models use data for calibration, they are not data-driven in the machine learning sense—lacking flexibility to adapt to unseen conditions without manual tuning. Building upon these modeling approaches, automated control systems have been increasingly adopted in greenhouse operations to maintain optimal environmental conditions [13]. Among advanced techniques, Model Predictive Control (MPC) stands out for its superior performance and energy efficiency relative to traditional methods [12]. The prediction model forms the cornerstone of any MPC strategy; its accuracy directly influences the quality of future state predictions and, consequently, the effectiveness of control actions. MPC typically employs analytical models—often in state-space form—to forecast system dynamics and determine optimal control inputs over a specified prediction horizon [11]. However, in practical applications, the development of first-principles models is frequently hindered by challenges such as incomplete system knowledge, complex parameter identification, and computational burdens that are incompatible with real-time operation. This has led to the emergence of data-driven black-box models as a viable alternative within the MPC framework. These models, trained exclusively on system input and output data, offer enhanced adaptability and computational efficiency. However, existing machine learning applications in greenhouse climate control, while promising, often struggle with key limitations, including poor generalization to unseen weather, sensitivity to noisy sensor data, and computational demands that impede real-time use. This research directly addresses this gap by integrating and systematically evaluating LSTM and GRU black-box models within the MPC framework for greenhouse control. The study focuses on assessing their predictive accuracy, robustness against environmental disturbances, and practical feasibility for real-time implementation under typical operational constraints and varying prediction horizons.

The rest of the paper is organized as follows: Section II presents a detailed review of related work and current trends in data-driven modeling and control for greenhouse and similar systems. Section III introduces the greenhouse system under study, detailing the dataset and key environmental variables used. Section IV explains the architecture, training, and evaluation of the LSTM and GRU models. Section V describes the integration of these mod-

els into the MPC framework, outlining the control objectives, constraints, and implementation strategy. Section VI presents the results of simulation experiments, including model performance metrics and a comparative analysis of control effectiveness. Finally, Section VII concludes the paper by summarizing key findings and outlining future research directions.

2. Related work

The growing interest in deep learning for time series forecasting has been driven by its powerful ability to model complex nonlinear relationships and automatically extract high-level features from raw data—capabilities that traditional methods often lack [18, 19]. Deep learning models are particularly well-suited for handling large-scale, high-dimensional, and multi-modal datasets, enabling them to uncover intricate patterns and significantly enhance prediction accuracy [20]. These advantages have made deep learning increasingly attractive for greenhouse modelling. For example, [21] developed a hybrid model that integrates attention mechanisms, convolutional neural networks (CNN), and LSTM networks to accurately predict temperature, humidity, and CO_2 levels in edible mushroom greenhouses. Similarly, [22] demonstrated that GRU can achieve accurate minimum temperature predictions even with a limited set of input variables, outperforming other models.

In parallel, the rapid advancement of artificial intelligence and data-driven modeling techniques has led to new and effective control strategies. For instance, [23], proposed a robust data-driven model predictive control framework that maintains high-precision temperature regulation and delivers notable energy savings under uncertain conditions. These findings underscore the potential of data-driven approaches in greenhouse climate management and highlight the need for continued research in this direction. The advent of deep learning has catalyzed extensive research focused on combining the robust representational power of deep neural networks with the fields of system modeling and control.

The stability of LSTM networks is a critical factor when they are used as predictive models within a MPC framework. the study [14] addressed this issue by establishing sufficient conditions to ensure Input-to-State Stability (ISS) and Incremental Input-to-State Stability (ISS) for LSTM networks. Leveraging these stability properties, they designed an observer with guaranteed convergence. Their study demonstrated that the resulting closed-loop system combining the observer and the MPC achieves asymptotic stability.

Several studies have explored the integration of neural networks into control frameworks to reduce the computational burden of Nonlinear MPC. In this regard, [15] proposed a method that leverages artificial neural networks to learn an affine parametrization of output predictions from data. This approach enables the efficient formulation and solution of Linear Time-Varying MPC (LTV-MPC) problems for nonlinear systems. Numerical simulations on the two-tank benchmark demonstrated that the method effectively captured system dynamics and delivered strong closed-loop performance with low computational cost. Similarly, [16] showed that stable GRU can be trained and incorporated into a Nonlinear MPC framework to achieve offset-free tracking of constant references with guaranteed closed-loop stability. In their approach, a GRU was trained to identify an unknown plant while ensuring stability, based on the conditions defined in [17]. The model was further augmented with an integrator to ensure offset-free tracking, and a converging state observer was designed for the augmented system. The proposed strategy demonstrated promising results when applied to a pH neutralization process benchmark.

The study [24] proposed a reduced-dimension optimization technique that integrates recurrent neural networks into nonlinear MPC, significantly lowering computational requirements and demonstrating real-time capability in chemical reactor simulations using parallel computing. Similarly, [25] presented an innovative MPC method combining online advanced trajectory linearization with LSTM and GRU predictors, enabling simple quadratic optimization while achieving prediction accuracy and control performance comparable to fully nonlinear MPC performance in real time. [26] developed a data-driven MPC framework for synchronous motor current control using an LSTM model; due to real-time constraints, the MPC computations were done offline, and a separate neural network was trained to efficiently execute control in real time. [27] proposed a robust MPC strategy leveraging LSTM-based predictions of a preceding vehicle’s speed and position to optimize fuel consumption while accounting for prediction errors. [28] combined physics-based and data-driven modeling within a real-time MPC system employing LSTMs for hydroelectric unit control, achieving improved accuracy and reduced optimization time compared to traditional methods. Lastly, [29] introduced a Practical Nonlinear MPC approach using LSTM networks for online nonlinear system prediction and local linearization, validated through simulations on neutralization reactors.

To conclude, the existing literature underscores the growing potential of deep

learning—particularly LSTM and GRU networks—for both greenhouse climate prediction and integration within MPC frameworks. These methods have demonstrated promising results across various domains by enhancing prediction accuracy, adaptability, and computational efficiency compared to traditional approaches. However, a significant gap remains in the systematic evaluation of deep recurrent models for real-time greenhouse climate control, especially under practical operational constraints and varying environmental disturbances. The novelty of this study lies in the design, integration, and evaluation of deep recurrent neural networks (LSTM and GRU) within a unified, real-time-capable MPC framework tailored to greenhouse systems. Unlike prior works that often rely on offline optimization, domain-specific configurations, or partial performance metrics, this research contributes:

- A comprehensive performance assessment of deep RNN-based models in MPC with respect to prediction accuracy, computational efficiency, robustness to external disturbances, and adaptability across different prediction horizons;
- An experimental workflow that emphasizes real-time implementation feasibility, using greenhouse-relevant input–output data to bridge the gap between theoretical model development and practical control deployment;
- A scalable modeling approach that minimizes reliance on system-specific tuning or first-principles knowledge, thereby enhancing transferability across greenhouse settings.

This study contributes significantly to combining deep learning with optimal control for protected agriculture, ultimately leading to more effective and resilient greenhouse management systems.

3. System Description and Data Acquisition

3.1. Greenhouse model

This study employs a validated dynamic model of a greenhouse environment initially developed by van Henten [30], which captures the complex interactions between indoor climate variables and lettuce crop growth. The model captures nonlinear dynamics and is widely recognized as a benchmark

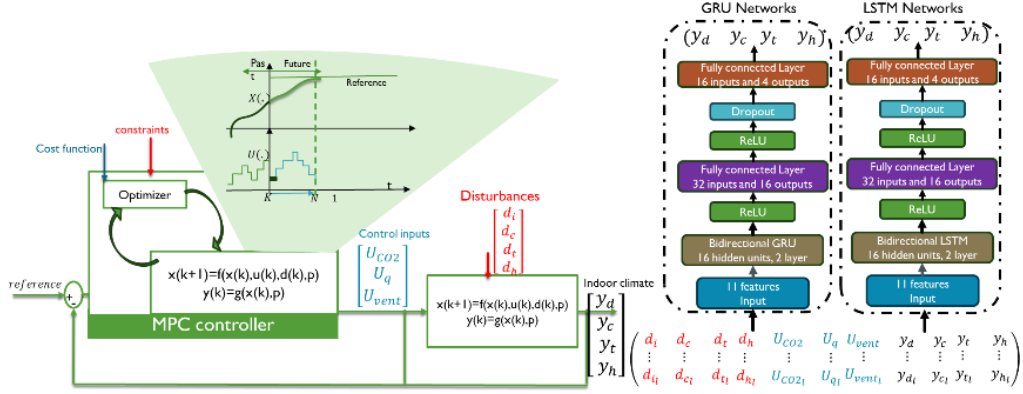


Figure 1: An overview of the MPC framework combined with LSTM and GRU neural networks is presented. The MPC controller generates control commands based on predictions from the van Henten [30] greenhouse model, external disturbances (solar radiation d_t , ambient temperature d_t , external CO₂ concentration d_c , and ambient humidity d_h), and reference trajectories. The LSTM and GRU networks are then trained on the data generated by this process. These networks learn to predict future greenhouse states—lettuce dry matter (y_d), indoor CO₂ concentration (y_c), indoor temperature (y_t), and indoor humidity (y_h)—based on historical data, disturbances, and previous control inputs. The modeling capabilities of the LSTM and GRU units to support the optimization process within the MPC loop is investigated.

for evaluating climate control strategies in greenhouse systems. For numerical implementation, the continuous-time formulation has been discretized using the explicit fourth-order Runge–Kutta method, with a fixed sampling interval of $h = 15$ minutes. The resulting discrete-time state-space model is defined as:

$$\mathbf{x}(k+1) = f(\mathbf{x}(k), \mathbf{u}(k), \mathbf{d}(k); \mathbf{p}), \quad (1)$$

$$\mathbf{y}(k) = g(\mathbf{x}(k); \mathbf{p}) \quad (2)$$

where $x(k) \in \mathbb{R}^4$ is the system state vector, $u(k) \in \mathbb{R}^3$ is the control input, $d(k) \in \mathbb{R}^4$ represents external weather disturbances, and $y(k) \in \mathbb{R}^4$ denotes the measurable output. The parameter vector $p \in \mathbb{R}^{28}$ encapsulates physical constants of the system. Table 1 provides an overview of the model variables and their physical interpretations.

3.2. Data Acquisition

The training data for both the LSTM and GRU models were generated through simulations using an MPC strategy [35] applied to the van Henten

Table 1: Model Variables and Descriptions

Category	Symbol	Description
State Variables (\mathbf{x})	x_W	Crop dry weight ($\text{kg}\cdot\text{m}^{-2}$)
	x_{CO_2}	Indoor CO_2 concentration ($\text{kg}\cdot\text{m}^{-3}$)
	x_T	Indoor temperature ($^{\circ}\text{C}$)
	x_h	Indoor absolute humidity ($\text{kg}\cdot\text{m}^{-3}$)
Control Inputs (\mathbf{u})	u_{CO_2}	CO_2 injection rate ($\text{mg}\cdot\text{m}^{-2}\cdot\text{s}^{-1}$)
	u_v	Ventilation rate ($\text{mm}\cdot\text{s}^{-1}$)
	u_q	Heating power supply ($\text{W}\cdot\text{m}^{-2}$)
Disturbances (\mathbf{d})	d_{Io}	Incoming solar radiation ($\text{W}\cdot\text{m}^{-2}$)
	d_{CO_2}	Outdoor CO_2 concentration ($\text{kg}\cdot\text{m}^{-3}$)
	d_T	Outdoor temperature ($^{\circ}\text{C}$)
	d_h	Outdoor absolute humidity ($\text{kg}\cdot\text{m}^{-3}$)
Measured Outputs (\mathbf{y})	y_W	Measured crop dry weight ($\text{kg}\cdot\text{m}^{-2}$)
	y_{CO_2}	Measured indoor CO_2 concentration (ppm)
	y_T	Measured indoor temperature ($^{\circ}\text{C}$)
	y_{RH}	Relative humidity (%)

greenhouse model described in Section 3.1. Real-world datasets that include synchronized outdoor disturbances, greenhouse control inputs, and resulting climate responses are scarce. To address this, we simulate control trajectories by applying the MPC controller to the greenhouse model under varying environmental conditions and greenhouse constraints. This method allows us to create realistic training scenarios that accurately reflect real-world greenhouse operations, all while ensuring variety and control.

Outdoor weather disturbance data—such as solar radiation ($\text{W}\cdot\text{m}^{-2}$), air temperature ($^{\circ}\text{C}$), CO_2 concentration ($\text{kg}\cdot\text{m}^{-3}$), and absolute humidity ($\text{kg}\cdot\text{m}^{-3}$)—were obtained from records collected between 2001 and 2020 at Schiphol Airport in the Netherlands [31]. For model training, data from the years 2007 to 2020 were used to capture a wide range of seasonal variability. The resulting dataset was split into two parts: 80% for training and 20% for testing. This partitioning ensures that the models are evaluated on unseen yet statistically similar conditions, supporting robust generalization performance.

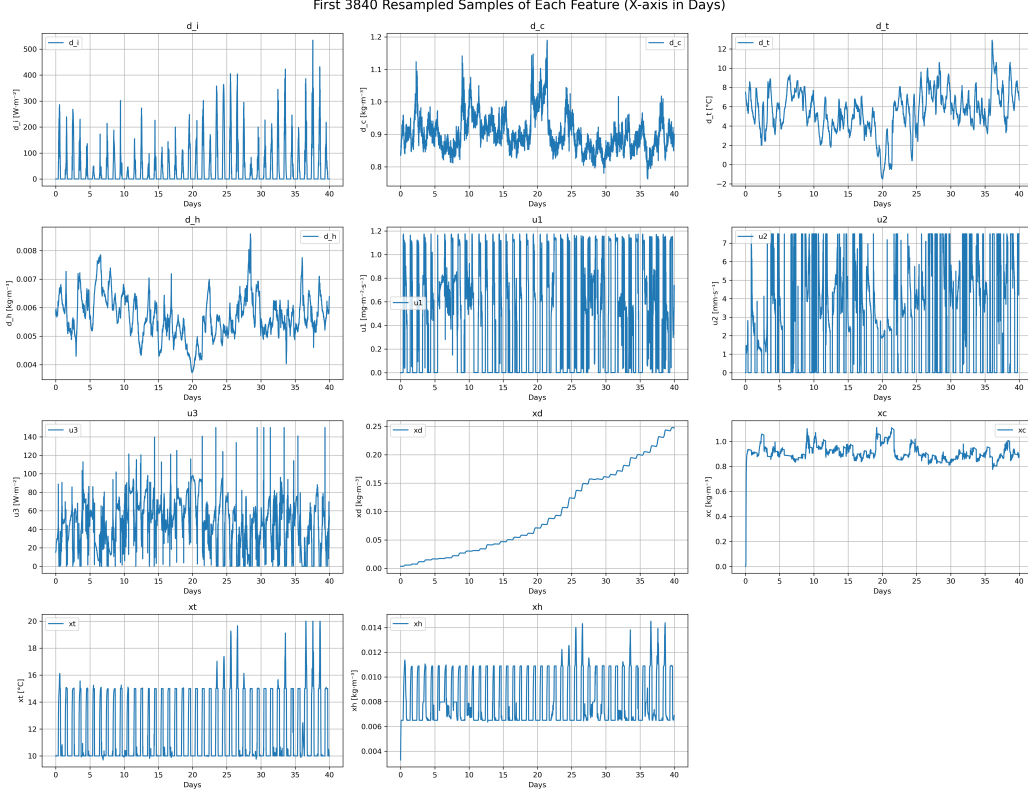


Figure 2: A sample of 3840 data points from the training dataset generated using the MPC strategy. The plot includes disturbances (solar radiation in $\text{W}\cdot\text{m}^{-2}$, outdoor temperature in $^{\circ}\text{C}$, outdoor CO₂ concentration, and outdoor humidity), control actions (CO₂ injection in $\text{mg}\cdot\text{m}^{-2}\cdot\text{s}^{-1}$, ventilation rate in $\text{mm}\cdot\text{s}^{-1}$, and heating system output in $\text{W}\cdot\text{m}^{-2}$), and greenhouse states (lettuce dry matter, indoor CO₂ concentration in $\text{kg}\cdot\text{m}^{-3}$, indoor temperature in $^{\circ}\text{C}$, and indoor humidity in $\text{kg}\cdot\text{m}^{-3}$). Time is expressed in days. These data were used to train the LSTM and GRU models.

4. Modeling and Control Framework

4.1. Predictive Model Based on LSTM and GRU Networks

RNNs, such as LSTM and GRU, are well-suited for modeling sequential data due to their capability to capture temporal dependencies. In greenhouse climate modeling, where environmental dynamics unfold over time, these models are particularly useful. Among RNN variants, LSTM networks stand out for their superior long-term memory through gating mechanisms and internal memory cells, enabling them to selectively retain and discard information.

At each time step t , the LSTM network processes three inputs: the current input sequence x_t , the previous hidden state h_{t-1} , and the previous cell state C_{t-1} . The update rules are as follows:

$$i_t = \sigma(W_i[h_{t-1}, x_t] + b_i) \quad (\text{input gate}) \quad (3)$$

$$\tilde{C}_t = \tanh(W_c[h_{t-1}, x_t] + b_c) \quad (\text{candidate cell state}) \quad (4)$$

$$f_t = \sigma(W_f[h_{t-1}, x_t] + b_f) \quad (\text{forget gate}) \quad (5)$$

$$C_t = f_t \odot C_{t-1} + i_t \odot \tilde{C}_t \quad (\text{cell state update}) \quad (6)$$

$$o_t = \sigma(W_o[h_{t-1}, x_t] + b_o) \quad (\text{output gate}) \quad (7)$$

$$h_t = o_t \odot \tanh(C_t) \quad (\text{hidden state}) \quad (8)$$

$$y_t = \phi(W_y h_t + b_y) \quad (\text{network output}) \quad (9)$$

Here, $\sigma(\cdot)$ and $\tanh(\cdot)$ represent the sigmoid and hyperbolic tangent activation functions, respectively, \odot denotes elementwise multiplication, and $\phi(\cdot)$ is the output activation function. Parameters W_* and b_* are learned using backpropagation through time (BPTT).

The GRU network simplifies the LSTM structure by combining the forget and input gates into a single update gate and merging the cell and hidden states. This results in fewer parameters and reduced training time:

$$z_t = \sigma(W_z[h_{t-1}, x_t] + b_z) \quad (\text{update gate}) \quad (10)$$

$$r_t = \sigma(W_r[h_{t-1}, x_t] + b_r) \quad (\text{reset gate}) \quad (11)$$

$$\tilde{h}_t = \tanh(W_h[r_t \odot h_{t-1}, x_t] + b_h) \quad (\text{candidate hidden state}) \quad (12)$$

$$h_t = (1 - z_t) \odot h_{t-1} + z_t \odot \tilde{h}_t \quad (\text{hidden state}) \quad (13)$$

$$y_t = \phi(W_y h_t + b_y) \quad (\text{network output}) \quad (14)$$

For both models, the input at each time step consists of external disturbances, past control inputs, and output measurements:

$$\begin{aligned} x_t = & [d(t), d(t-1), \dots, d(t-l_d); \\ & u(t), u(t-1), \dots, u(t-l_u); \\ & y(t), y(t-1), \dots, y(t-l_y)], \end{aligned}$$

where l_d , l_u , and l_y denote the number of historical time steps for disturbances, control inputs, and output variables, respectively. In this study,

we systematically benchmark the effect of different historical window sizes ($l_d = l_u = l_y = \{6, 12, 18, 24\}$) on prediction accuracy. This input sequence is used to predict the immediate next output of the system, i.e., the system behavior 15 minutes (900 seconds) ahead.

4.1.1. Network Architecture

The implemented LSTM and GRU networks share a similar architecture tailored to greenhouse climate prediction, each consisting of two bidirectional layers with a hidden size of 16 units per direction, effectively producing a 32-dimensional output per time step. The input to the networks has 11 features, representing external disturbances, control inputs, and output measurements. The output from the final time step of the recurrent layers is fed through two fully connected layers, where the first reduces the dimension from 32 to 16 with a ReLU activation and dropout, and the second maps to 4 predicted output features. This design enables effective sequence modeling of greenhouse climate dynamics for accurate system output prediction.

4.1.2. Training Objective

The model is trained to minimize the mean squared error over a single-step prediction horizon $T_p = 1$:

$$\mathcal{L} = \left\| R(t) - \hat{Y}(t) \right\|_2^2,$$

where $R(t) = r(t+1)$ is the target value at the immediate next time step, and $\hat{Y}(t) = \hat{y}(t+1)$ denotes the predicted output for that next step.

4.1.3. Advantages

The primary benefits of using LSTM and GRU for predictive modeling in greenhouse systems are twofold: (1) their gating mechanisms enable the extraction of meaningful temporal features from sequential input data, which aligns well with the feedback nature of MPC, and (2) unlike classical predictive methods (e.g., AutoRegressive Integrated Moving Average (ARIMA)), they do not rely on a fixed-order assumption, making them more robust and generalizable to various system dynamics.

4.2. Online Model Predictive Control Framework

In greenhouse climate management, key system states such as indoor air temperature, absolute humidity, and CO₂ concentration are directly tied to

crop productivity. Maintaining these states within biologically safe and effective ranges is essential: extreme temperatures can halt plant growth, and excessive humidity fosters mold, reducing both yield and quality. As a result, constraints are applied to these states to safeguard plant health and optimize lettuce production. The primary control variables include heating, ventilation, and CO₂ enrichment, while external disturbances comprise solar radiation, ambient temperature, ambient humidity, and ambient CO₂ levels. Building on the LSTM and GRU models described in section 4.1, we implement a predictive control strategy using the respective trained LSTM and GRU networks. This predictive control follows a receding horizon approach, in which the system state is measured at each time step and used to update the model’s initial condition. An optimization problem is then solved over a finite prediction horizon N_p , aiming to minimize a cost function that balances crop yield and energy consumption. Only the first control input from the optimized sequence is applied, after which the process is repeated at the next time step using the newly measured state.

The optimization problem seeks to determine the control inputs that minimize a weighted cost function:

$$V(u(k), y(k)) = -q_{y_d} \cdot y_1(k) + \sum_{j=1}^3 q_{u_j} \cdot u_j(k), \quad (15)$$

In this study, $q_{y_d} = 1000$ and $q_{u_j} = \{10, 1, 1\}$ are tunable weights that were selected to balance the relative importance of the tracking error and control effort in the cost function. This cost function captures the trade-off between maximizing lettuce yield and minimizing energy usage. The optimization is subject to the dynamic system behavior modeled by the trained LSTM or GRU networks, as well as constraints on control inputs, their rate of change, and time-varying output bounds. Notably, the indoor temperature constraints vary throughout the day to reflect crop-specific day–night requirements [32]. These constraints ensure that the controller operates within safe and biologically meaningful ranges while optimizing overall greenhouse performance. The optimization problem is subject to the following constraints on control inputs and system outputs:

$$\begin{aligned} \mathbf{u}_{\min} &= \begin{bmatrix} 0 \\ 0 \\ 0 \end{bmatrix}, \quad \mathbf{u}_{\max} = \begin{bmatrix} 1.2 \\ 7.5 \\ 150 \end{bmatrix}, \quad \Delta \mathbf{u}_{\max} = \frac{1}{10} \cdot \mathbf{u}_{\max}, \\ \mathbf{y}_{\min}(k) &= \begin{bmatrix} 0 \\ 0 \\ f_{y_t, \min}(k) \\ 50 \end{bmatrix}, \quad \mathbf{y}_{\max}(k) = \begin{bmatrix} \infty \\ 1000 \\ f_{y_t, \max}(k) \\ 85 \end{bmatrix}, \end{aligned} \quad (16)$$

where the time-varying temperature bounds are given by:

$$f_{y_3, \min}(k) = \begin{cases} 10, & \text{if } d_i(k_0) < 10 \\ 15, & \text{otherwise} \end{cases}, \quad (17)$$

$$f_{y_3, \max}(k) = \begin{cases} 15, & \text{if } d_i(k_0) < 10 \\ 20, & \text{otherwise} \end{cases}. \quad (18)$$

Additionally, CO₂ injection is restricted to daytime hours. This is enforced by setting the third control input to zero outside daytime:

$$u_3(k) = \begin{cases} 0, & \text{if } d_i(k_0) < 10 \\ u_3(k), & \text{otherwise} \end{cases}. \quad (19)$$

These constraints ensure biologically appropriate greenhouse conditions, including diurnal temperature variation and restricting CO₂ enrichment to periods when photosynthesis can actively benefit from it. The optimization problem described in equations 15–19 is solved in PYTHON using the open-source tools CasADi [36], the IPOPT solver [37], and the L4casadi framework [38].

5. Experimental Results and Performance Evaluation

In this experiment, we trained and evaluated both LSTM and GRU neural network models to predict greenhouse environmental conditions based on historical data and control inputs. The training dataset, derived from a real greenhouse model controlled by an MPC, was resampled to a 15-minute interval and normalized to the unit range. Both models were implemented in PyTorch with a bidirectional architecture consisting of two layers and a

hidden size of 16 units. The input sequences included 11 features over sliding windows of various lengths (6, 12, 18, and 24), and the target outputs comprised four key greenhouse variables. The training process employed the Adam optimizer with a learning rate of 3×10^{-5} and a StepLR scheduler, and training was conducted over 15 epochs. For each model, experiments were conducted with different batch sizes (8, 16, and 32) to identify the best configuration. Model performance was evaluated using Mean Squared Error (MSE) and Root Mean Squared Error (RMSE) metrics on a separate test set composed of MPC-generated trajectories as shown on figure 3. The evaluation involved inverse-scaling the model outputs and comparing them to actual greenhouse measurements. The GRU model achieved its best performance with a window size of 24 and a batch size of 8 (MSE = 0.0162, RMSE = 0.1271), while the LSTM performed best with a window size of 24 and a batch size of 16 (MSE = 0.0167, RMSE = 0.1293). These results highlight the importance of selecting an appropriate temporal context and batch size for optimal sequence modeling in data-driven greenhouse climate prediction. Table 2 summarizes the results. The best-performing configurations for each model are highlighted in bold.

Table 2: Comparison of GRU and LSTM model performance across different batch and window sizes

Model	Batch Size	Window Size	MSE	RMSE
GRU	8	24	0.0162	0.1271
		18	0.0192	0.1387
		12	0.0516	0.2270
		6	0.0279	0.1672
	16	24	0.0179	0.1339
		18	0.0900	0.1380
		12	0.0224	0.1498
		6	0.0233	0.1526
	32	24	0.0172	0.1312
		18	0.0180	0.1341
		12	0.0297	0.1724
		6	0.0165	0.1283
LSTM	8	24	0.0274	0.1657
		18	0.0300	0.1733
		12	0.0212	0.1457
		6	0.0660	0.2568
	16	24	0.0167	0.1293
		18	0.0255	0.1590
		12	0.0189	0.1375
		6	0.0188	0.1372
	32	24	0.0218	0.1478
		18	0.0209	0.1445
		12	0.0224	0.1497
		6	0.0269	0.1640

As shown in Figure 3, the GRU model with a window size of 24 closely tracks the actual climate response, confirming its suitability for predictive control applications.

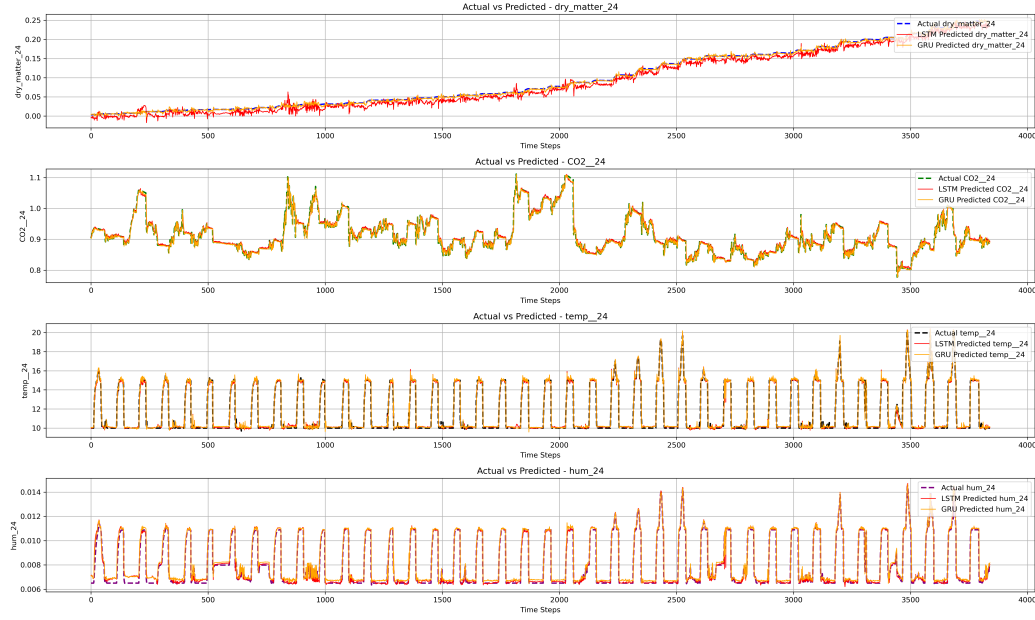


Figure 3: Prediction performance of the GRU model with window size 24 compared to the actual system response. The plot illustrates the model's ability to follow the true dynamics of the greenhouse climate system.

Figure 4 illustrates the time-series evolution of key variables within a greenhouse environment managed by various control strategies, including GRU-based controllers with prediction horizons ranging from 1.5 hours (6 time steps) to 7.5 hours (30 time steps), as well as a baseline MPC controller with a 6-hour horizon (24 time steps). The subplots, arranged from top to bottom, depict: (1) crop dry matter accumulation, (2) CO₂ injection rate, (3) indoor CO₂ concentration, (4) outdoor CO₂ levels, (5) heating input, (6) ventilation rate, (7) indoor air temperature including comfort/control bounds, (8) outdoor temperature, (9) solar irradiance, (10) indoor relative humidity, and (11) outdoor relative humidity. Differences between control strategies are distinguished by unique line styles and colors. The figure demonstrates each controller's ability to regulate the greenhouse climate in response to external disturbances while optimizing conditions for plant growth.

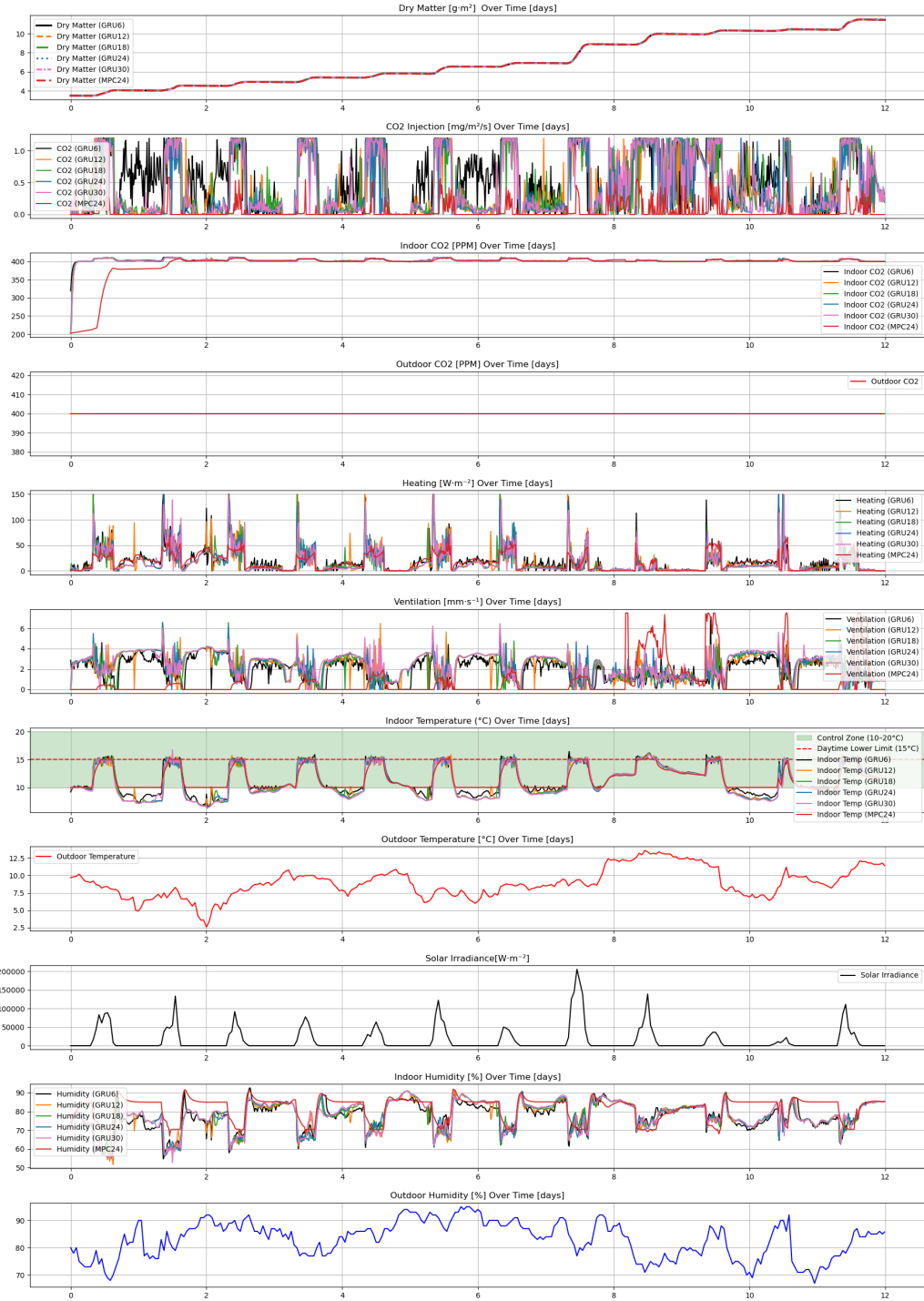


Figure 4: Temporal evolution of greenhouse internal parameters, control actions, and external environmental disturbances under different predictive control strategies. The plots illustrate dry matter production, indoor CO₂ concentration, temperature, humidity, heating, ventilation, and the effects of outdoor conditions such as solar irradiance, CO₂, and temperature.



Figure 5: Temporal evolution of greenhouse internal parameters, control actions, and external environmental disturbances under different predictive control strategies. The plots illustrate dry matter production, indoor CO₂ concentration, temperature, humidity, heating, ventilation, and the effects of outdoor conditions such as solar irradiance, CO₂, and temperature.

Table 3: Violation Metrics, Economic Indicators, and Processing Time for LSTM, GRU, and MPC Models

Model	Temp. Viol. (%)	Day Temp. (°C)	Night Temp. (°C)	Hum. Viol. (%)	Hum. Mean (%)	EPI (Hf m ⁻²)	Dry Matter (g m ⁻²)	Processing Time (s)
LSTM6	45.66	0.93	1.44	17.71	1.70	1.65	11.44	27
LSTM12	52.52	0.78	1.65	24.31	1.80	1.70	11.46	68
LSTM18	56.68	0.83	1.63	22.31	1.68	1.70	11.46	159
LSTM24	59.38	0.77	1.59	23.52	1.61	1.70	11.47	360
LSTM30	58.68	0.82	1.61	23.61	1.48	1.70	11.47	502
GRU6	49.65	0.64	0.99	15.45	1.76	1.63	11.44	19
GRU12	59.55	0.69	1.34	16.67	1.76	1.68	11.46	66
GRU18	61.11	0.64	1.39	16.49	1.86	1.69	11.47	147
GRU24	62.93	0.71	1.47	17.62	1.85	1.71	11.47	254
GRU30	63.63	0.79	1.50	17.80	1.92	1.70	11.47	422
MPC24	50.61	1.18	0.00	54.77	0.93	1.86	11.44	0.01

6. Discussion

This section presents a comprehensive comparison of the LSTM-, GRU-, and MPC-based controllers. The analysis centers on several key aspects: climate constraint violations, which refer to any instances where the system’s operation deviated from pre-established environmental limits or targets (e.g., maximum and minimum allowable humidity or the desired temperature ranges); economic outcomes; crop productivity; and computational cost. The metrics detailed in Table 3 provide the foundation for this comparison.

6.1. Control Performance.

To quantitatively evaluate and compare the performance of the three controllers, we adopt a multi-criteria framework based on thermal comfort, humidity regulation, and economic productivity. Each metric is defined below to standardize interpretation.

6.1.1. Economic Performance Index (EPI).

The EPI captures the net profit over time, balancing crop revenue against heating and CO₂ enrichment costs. It is defined as:

$$\begin{aligned}
 \text{EPI} &= \frac{1}{N} \sum_{k=1}^N [\text{Revenue}(k) - \text{Cost}_{\text{CO}_2}(k) - \text{Cost}_{\text{heat}}(k)] \\
 &= (c_{\text{pri1}} + c_{\text{pri2}} \cdot y_{1\text{ kg}}) - \sum (c_q \cdot u_q + c_{\text{CO}_2} \cdot u_{\text{CO}_2}) \cdot h
 \end{aligned}$$

Here, $y_{1\text{ kg}}$ denotes dry matter yield (kg·m⁻²), c_{pri1} and c_{pri2} are crop pricing coefficients, and c_q , c_{CO_2} represent operational cost factors for heating and CO₂, respectively. The variable h is the time interval, and N is the total number of simulation steps. The parameters used to calculate the Economic Performance Index (EPI) include the CO₂ enrichment cost coefficient c_{CO_2} =

$42 \times 10^{-2} \text{ Hf kg}^{-1}$, the heating cost coefficient $c_q = 6.35 \times 10^{-9} \text{ Hf J}^{-1}$, and the crop pricing coefficients $c_{\text{pri1}} = 1.8 \text{ Hf m}^{-2}$ and $c_{\text{pri2}} = 16 \text{ Hf kg}^{-1}$, as proposed by [35].

6.1.2. Thermal Violations

Temperature constraint violations are evaluated based on time-of-day irradiance conditions, reflecting operational greenhouse control guidelines:

- **Nighttime violation** If irradiance is low and temperature is below 10°C :

$$\text{if } d_i < 10 \text{ and } y_t < 10 \implies \text{violation magnitude} = 10 - y_t$$

- **Daytime violation** If irradiance is high and temperature is below 15°C :

$$\text{if } d_i \geq 10 \text{ and } y_t < 15 \implies \text{violation magnitude} = 15 - y_t$$

The total number of thermal violations is given by V_T , the count of time steps where either of the above conditions is violated.

6.1.3. Humidity Violations

Humidity constraint violations are defined as:

$$y_h > 85 \implies \text{violation magnitude} = y_h - 85$$

with V_H representing the total count of humidity violations during the simulation.

6.1.4. Violation Rates:

For standardized comparison, violation rates are reported as percentages:

- **Temperature Violation Rate (%)**:

$$\text{Violation Rate}_T = \frac{V_T}{N} \times 100$$

- **Humidity Violation Rate (%)**:

$$\text{Violation Rate}_H = \frac{V_H}{N} \times 100$$

From Table 3, both LSTM and GRU controllers show varying degrees of constraint violations depending on prediction horizon. GRU6 demonstrates the best performance in temperature and humidity regulation, while LSTM24 and GRU24 strike a favorable balance between control quality and economic outcomes. The MPC controller excels in temperature control—registering zero nighttime violations—but performs poorly in humidity regulation, with a 54.77% violation rate.

6.2. *Economic Performance and Crop Productivity*

Despite higher violation rates, the data-driven models (especially GRU24 and LSTM24) approach the economic performance of MPC. The MPC controller yields the highest EPI (1.86 Hfl m⁻²), but GRU24 and LSTM24 also achieve competitive values (1.71 and 1.70 Hfl m⁻², respectively), affirming their cost-effectiveness under learned greenhouse dynamics.

Dry matter accumulation remains effectively constant across all models, indicating that violations—particularly at night—do not significantly impair daytime photosynthesis, which drives biomass production.

6.3. *Model Efficiency and Practical Trade-Offs*

GRU networks exhibit superior computational efficiency. For instance, GRU24 completes execution in 254 seconds compared to LSTM24’s 360 seconds. This efficiency is critical for real-time greenhouse control, where inference speed affects responsiveness. Furthermore, GRU’s simpler architecture enables faster convergence during training without sacrificing prediction accuracy.

While MPC remains computationally trivial (0.01 seconds), its rule-based structure lacks adaptability, which compromises its performance in dynamically varying humidity conditions.

6.4. *Summary and Implications*

The results demonstrate that GRU-based predictive controllers provide an attractive balance of adaptability, performance, and efficiency for practical

deployment in greenhouse environments. While MPC still holds advantages in terms of strict constraint adherence and execution speed, its inflexibility to environmental changes and poorer humidity regulation are significant limitations.

Table 4: Comparison of MPC and GRU-based Controllers in Greenhouse Control

Feature	MPC24	GRU-based Controllers
Climate Regulation	Good, but less effective humidity control	Best performance with GRU6
Economic Outcome	Best (highest EPI)	Near-optimal with GRU24
Adaptability to Environment	Low (inflexible)	High (adaptive)
Computation Efficiency	Highest (minimal processing time)	Moderate to high
Overall Balance	Strong in speed and economics	Best overall balance with GRU24

Overall, GRU-based control emerges as a highly promising alternative for intelligent greenhouse automation, combining high predictive accuracy with practical real-time deployment potential.

7. Conclusions

This study has demonstrated the effectiveness of data-driven predictive control strategies, specifically using GRU and LSTM neural networks, for optimizing greenhouse climate regulation. By leveraging historical data and capturing temporal dynamics, both models proved capable of maintaining environmental conditions within acceptable physiological bounds. However, the GRU-based predictive controller consistently outperformed its LSTM counterpart in terms of computational efficiency, faster training convergence, and slightly better violation metrics.

The GRU controller reduced temperature and humidity violations by up to 5%, while achieving a 40% reduction in processing time without compromising crop yield or economic performance. These advantages make GRU

particularly well-suited for real-time deployment in greenhouse systems where computational resources and responsiveness are critical.

Overall, this research validates the potential of GRU-based predictive control as a practical and scalable solution for smart agriculture applications, enabling more sustainable and energy-efficient food production. Future work may explore hybrid architectures, integration with reinforcement learning, and application to multi-crop or multi-zone greenhouses to further enhance performance and adaptability.

Data Availability

Data will be made available on request.

Acknowledgments

This research was funded by the Engineering and Physical Sciences Research Council (EPSRC) and the AgriFoRwArdS Centre for Doctoral Training (CDT) under grant number EP/S023917/1.

Appendix: Lettuce Greenhouse Model

The dynamic model used to represent the lettuce greenhouse environment is described by the following system of differential equations:

$$\begin{aligned}\frac{dx_1(t)}{dt} &= p_{1,1} \phi_{\text{phot},c}(t) - p_{1,2} \frac{x_1(t)^2 x_3(t)}{10^{5/2}}, \\ \frac{dx_2(t)}{dt} &= \frac{1}{p_{2,1}} \left(-\phi_{\text{phot},c}(t) + p_{2,2} \frac{x_1(t)^2 x_3(t)}{10^{5/2}} + u_1(t) \cdot 10^{-6} - \phi_{\text{vent},c}(t) \right), \\ \frac{dx_3(t)}{dt} &= \frac{1}{p_{3,1}} \left(u_3(t) - (p_{3,2} u_2(t) \cdot 10^{-3} + p_{3,3})(x_3(t) - d_3(t)) + p_{3,4} d_1(t) \right), \\ \frac{dx_4(t)}{dt} &= \frac{1}{p_{4,1}} (\phi_{\text{transp},h}(t) - \phi_{\text{vent},h}(t)).\end{aligned}$$

The supporting functions are defined as:

$$\begin{aligned}
\phi_{\text{phot},c}(t) &= (1 - e^{-p_{1,3}x_1(t)}) \cdot \frac{p_{1,4}d_1(t) (-p_{1,5}x_3(t)^2 + p_{1,6}x_3(t) - p_{1,7}) (x_2(t) - p_{1,8})}{\phi(t)}, \\
\phi(t) &= p_{1,4}d_1(t) + (-p_{1,5}x_3(t)^2 + p_{1,6}x_3(t) - p_{1,7}) (x_2(t) - p_{1,8}), \\
\phi_{\text{vent},c}(t) &= (u_2(t) \cdot 10^{-3} + p_{2,3}) (x_2(t) - d_2(t)), \\
\phi_{\text{vent},h}(t) &= (u_2(t) \cdot 10^{-3} + p_{2,3}) (x_4(t) - d_4(t)), \\
\phi_{\text{transp},h}(t) &= p_{4,2} (1 - e^{-p_{1,3}x_1(t)}) \left(\frac{p_{4,3}}{p_{4,4}(x_3(t) + p_{4,5})} \exp \left(\frac{p_{4,6}x_3(t)}{x_3(t) + p_{4,7}} \right) - x_4(t) \right).
\end{aligned}$$

Here, $t \in \mathbb{R}$ denotes continuous time. The terms $\phi_{\text{phot},c}(t)$, $\phi_{\text{vent},c}(t)$, $\phi_{\text{transp},h}(t)$, and $\phi_{\text{vent},h}(t)$ represent: - the gross canopy photosynthesis rate, - CO₂ exchange through the ventilation system, - canopy transpiration rate, and - H₂O exchange through the ventilation system, respectively.

The output (measurement) equations are given as:

$$\begin{aligned}
y_1(t) &= 10^3 \cdot x_1(t) \quad (\text{g m}^{-2}), \\
y_2(t) &= 10^3 \cdot p_{2,4} \cdot \frac{(x_3(t) + p_{2,5})}{p_{2,6}p_{2,7}} \cdot x_2(t) \quad (\text{ppm}), \\
y_3(t) &= x_3(t) \quad (^\circ\text{C}), \\
y_4(t) &= 10^2 \cdot p_{2,4} \cdot (x_3(t) + p_{2,5}) \cdot \frac{1}{11} \cdot \exp \left(\frac{p_{4,8}x_3(t)}{x_3(t) + p_{4,9}} \right) \cdot x_4(t) \quad (\%).
\end{aligned}$$

The model parameters $p_{i,j}$ follow the definitions provided in [30] and are listed in Table .5. A fourth-order explicit Runge–Kutta method is used for discretization of the continuous model, leading to the form presented.

Table .5: Model parameters used in the simulation.

Parameter	Value	Parameter	Value
$p_{1,1}$	0.544	$p_{1,2}$	$2.65 \cdot 10^{-7}$
$p_{1,3}$	53	$p_{1,4}$	$3.55 \cdot 10^{-9}$
$p_{1,5}$	$5.11 \cdot 10^{-6}$	$p_{1,6}$	$2.3 \cdot 10^{-4}$
$p_{1,7}$	$6.29 \cdot 10^{-4}$	$p_{1,8}$	$5.2 \cdot 10^{-5}$
$p_{2,1}$	4.1	$p_{2,2}$	$4.87 \cdot 10^{-7}$
$p_{2,3}$	$7.5 \cdot 10^{-6}$		
$p_{3,1}$	$3 \cdot 10^4$	$p_{3,2}$	1290
$p_{3,3}$	6.1	$p_{3,4}$	0.2
$p_{4,1}$	4.1	$p_{4,2}$	0.0036
$p_{4,3}$	9348	$p_{4,4}$	8314
$p_{4,5}$	273.15	$p_{4,6}$	17.4
$p_{4,7}$	239		

References

- [1] López-Cruz, I.L., Fitz-Rodríguez, E., Salazar-Moreno, R., Rojano-Aguilar, A., Kacira, M., et al. Development and analysis of dynamical mathematical models of greenhouse climate: A review. *Eur. J. Hortic. Sci.*, 83(5):269–280, 2018.
- [2] Katzin, D., Van Henten, E.J., and Van Mourik, S. Process-based greenhouse climate models: Genealogy, current status, and future directions. *Agricultural Systems*, 198:103388, 2022.
- [3] Van Straten, G., and Van Henten, E.J. Optimal greenhouse cultivation control: survey and perspectives. *IFAC Proceedings Volumes*, 43(26):18–33, 2010.
- [4] United Nations. Growing at a slower pace, world population is expected to reach 9.7 billion in 2050 and could peak at nearly 11 billion around 2100. Department of Economic and Social Affairs, 2019.
- [5] FAO. The future of food and agriculture—Alternative pathways to 2050. *Glob. Perspect. Stud.*, 2018.
- [6] FOOD, REPURPOSING and AFFORDABLE, HEALTHY DIETS MORE. Food security and nutrition in the World, 2022.

- [7] Marcelis, L.F.M., Costa, J.M., and Heuvelink, E. Achieving sustainable greenhouse production: present status, recent advances and future developments. *Achieving sustainable greenhouse cultivation*, pp. 1–14, 2019.
- [8] Stanghellini, C. Horticultural production in greenhouses: efficient use of water. In: *International Symposium on Growing Media and Soilless Cultivation 1034*, pp. 25–32, 2013.
- [9] Graamans, L., Baeza, E., Van Den Dobbelsteen, A., Tsafaras, I., and Stanghellini, C. Plant factories versus greenhouses: Comparison of resource use efficiency. *Agricultural Systems*, 160:31–43, 2018.
- [10] De Gelder, A., Dieleman, J.A., Bot, G.P.A., and Marcelis, L.F.M. An overview of climate and crop yield in closed greenhouses. *The Journal of Horticultural Science and Biotechnology*, 87(3):193–202, 2012.
- [11] Bersani, C., Ouammi, A., Sacile, R., and Zero, E. Model predictive control of smart greenhouses as the path towards near zero energy consumption. *Energies*, 13(14):3647, 2020.
- [12] Afram, A., and Janabi-Sharifi, F. Theory and applications of HVAC control systems—A review of model predictive control (MPC). *Building and Environment*, 72:343–355, 2014.
- [13] Maraveas, C., Karavas, C.S., Loukatos, D., Bartzanas, T., Arvanitis, K.G., and Symeonaki, E. Agricultural greenhouses: Resource management technologies and perspectives for zero greenhouse gas emissions. *Agriculture*, 13(7):1464, 2023.
- [14] Terzi, E., Bonassi, F., Farina, M., and Scattolini, R. Learning model predictive control with long short-term memory networks. *International Journal of Robust and Nonlinear Control*, 31(18):8877–8896, 2021.
- [15] Masti, D., Smarra, F., D’Innocenzo, A., and Bemporad, A. Learning affine predictors for MPC of nonlinear systems via artificial neural networks. *IFAC-PapersOnLine*, 53(2):5233–5238, 2020.
- [16] Bonassi, F., da Silva, C.F.O., and Scattolini, R. Nonlinear MPC for offset-free tracking of systems learned by GRU neural networks. *IFAC-PapersOnLine*, 54(14):54–59, 2021.

- [17] Bonassi, F., Farina, M., and Scattolini, R. On the stability properties of gated recurrent units neural networks. *Systems & Control Letters*, 157:105049, 2021.
- [18] Li, H., Guo, Y., Zhao, H., Wang, Y., and Chow, D. Towards automated greenhouse: A state of the art review on greenhouse monitoring methods and technologies based on internet of things. *Computers and Electronics in Agriculture*, 191:106558, 2021.
- [19] Torres, J.F., Hadjout, D., Sebaa, A., Martínez-Álvarez, F., and Troncoso, A. Deep learning for time series forecasting: a survey. *Big Data*, 9(1):3–21, 2021.
- [20] Liu, G., Zhong, K., Li, H., Chen, T., and Wang, Y. A state of art review on time series forecasting with machine learning for environmental parameters in agricultural greenhouses. *Information Processing in Agriculture*, 11(2):143–162, 2024.
- [21] Huang, S., Liu, Q., Wu, Y., Chen, M., Yin, H., and Zhao, J. Edible mushroom greenhouse environment prediction model based on attention cnn-lstm. *Agronomy*, 14(3):473, 2024.
- [22] He, Z., Jiang, T., Jiang, Y., Luo, Q., Chen, S., et al. Gated recurrent unit models outperform other machine learning models in prediction of minimum temperature in greenhouse based on local weather data. *Computers and Electronics in Agriculture*, 202:107416, 2022.
- [23] Mahmood, F., Govindan, R., Bermak, A., Yang, D., and Al-Ansari, T. Data-driven robust model predictive control for greenhouse temperature control and energy utilisation assessment. *Applied Energy*, 343:121190, 2023.
- [24] Doncevic, D.T., Schweidtmann, A.M., Vaupel, Y., Schäfer, P., Caspari, A., and Mitsos, A. Deterministic global nonlinear model predictive control with neural networks embedded. *IFAC-PapersOnLine*, 53(2):5273–5278, 2020.
- [25] Zarzycki, K., and Ławryńczuk, M. Advanced predictive control for GRU and LSTM networks. *Information Sciences*, 616:229–254, 2022.

- [26] Hammoud, I., Hentzelt, S., Oehlschlaegel, T., and Kennel, R. Learning-based model predictive current control for synchronous machines: An LSTM approach. *European Journal of Control*, 68:100663, 2022.
- [27] Baby, T.V., Sotoudeh, S.M., and HomChaudhuri, B. Data-driven prediction and predictive control methods for eco-driving in production vehicles. *IFAC-PapersOnLine*, 55(37):633–638, 2022.
- [28] Ye, S., Wang, C., Wang, Y., Lei, X., Wang, X., and Yang, G. Real-time model predictive control study of run-of-river hydropower plants with data-driven and physics-based coupled model. *Journal of Hydrology*, 617:128942, 2023.
- [29] Schwedersky, B.B., Flesch, R.C.C., and Dangui, H.A.S. Practical nonlinear model predictive control algorithm for long short-term memory networks. *IFAC-PapersOnLine*, 52(1):468–473, 2019.
- [30] Van Henten, E.J. *Greenhouse climate management: an optimal control approach*. Wageningen University and Research, 1994.
- [31] Van Laatum, B., Van Henten, E.J., and Boersma, S. GreenLight-Gym: Reinforcement learning benchmark environment for control of greenhouse production systems.
- [32] Seginer, I., Gary, C., and Tchamitchian, M. Optimal temperature regimes for a greenhouse crop with a carbohydrate pool: A modelling study. *Scientia Horticulturae*, 60(1–2):55–80, 1994.
- [33] Choab, N., Allouhi, A., El Maakoul, A., Kousksou, T., Saadeddine, S., and Jamil, A. Review on greenhouse microclimate and application: Design parameters, thermal modeling and simulation, climate controlling technologies. *Solar Energy*, 191:109–137, 2019.
- [34] Norton, T., Sun, D.-W., Grant, J., Fallon, R., and Dodd, V. Applications of computational fluid dynamics (CFD) in the modelling and design of ventilation systems in the agricultural industry: A review. *Bioresource Technology*, 98(12):2386–2414, 2007.
- [35] Morcego, B., Yin, W., Boersma, S., Van Henten, E., Puig, V., and Sun, C. Reinforcement learning versus model predictive control on greenhouse

- climate control. *Computers and Electronics in Agriculture*, 215:108372, 2023.
- [36] Andersson, J.A.E., Gillis, J., Horn, G., Rawlings, J.B., and Diehl, M. CasADi: a software framework for nonlinear optimization and optimal control. *Mathematical Programming Computation*, 11:1–36, 2019.
 - [37] Wächter, A., and Biegler, L.T. On the implementation of an interior-point filter line-search algorithm for large-scale nonlinear programming. *Mathematical Programming*, 106:25–57, 2006.
 - [38] Salzmann, T., Arrizabalaga, J., Andersson, J., Pavone, M., and Ryll, M. Learning for CasADi: Data-driven models in numerical optimization. In: *6th Annual Learning for Dynamics & Control Conference*, pp. 541–553, 2024.